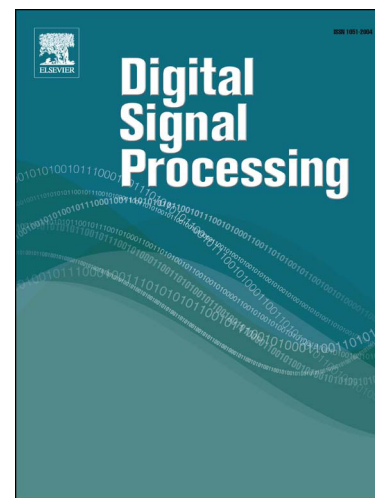# Accepted Manuscript

Joint Quality Enhancement and Power Control for Wireless Visual Sensor Networks based on the Nash Bargaining Solution

Eftychia G. Datsika, Angeliki V. Katsenou, Lisimachos P. Kondi, Evangelos Papapetrou, Konstantinos E. Parsopoulos

Joint Quality Enhancement and Power Control for Wireless Visual Sensor Networks based on the Nash Bargaining Solution

Eftychia G. Datsika[†], Angeliki V. Katsenou[§1], Lisimachos P. Kondi[‡], Evangelos Papapetrou[‡] and Konstantinos E. Parsopoulos[‡]

[†]*IQUADRAT Informatica S. L., Barcelona, Spain*
[§]*Department of Electrical and Electronic Engineering, University of Bristol, BS8 1UB, Bristol, United Kingdom*
[‡]*Department of Computer Science and Engineering, University of Ioannina, GR-45110, Ioannina, Greece*

Abstract

We propose a cooperative method for resource allocation with power control in a multihop Direct Sequence Code Division Multiple Access *Wireless Visual Sensor Network* (WVSN). Typical multihop WVSNs consist of visual sensors that record different scenes and relay nodes that retransmit video data until the base station is reached. The error prone wireless environment contributes to the end-to-end video quality degradation. Moreover, the limited battery life span of the network nodes poses challenges on the management of power consumption. The different resource requirements of the WVSN nodes necessitate a quality-driven and power-aware resource allocation mechanism. We formulate the joint Quality Enhancement and Power Control problem based on a utility function that reflects both the benefit in terms of video quality and the cost in terms of transmission power. This function is employed by the Nash Bargaining Solution, which achieves higher fairness in terms of end-to-end video quality among all nodes. For the fairness assessment, a new metric is introduced. The experiments demonstrate the effectiveness of the proposed approach and explain the video quality-power consumption tradeoff as well as the resulting fairness-power consumption tradeoff.

[1]Corresponding Author Contact Details:
e-mail: akatsenou@gmail.com, phone: +302651008904, fax: +302651008890

1. Introduction

Recent advances in video coding technologies and wireless communications have provided several applications and systems, such as healthcare, public safety systems, environmental monitoring and traffic analysis [1]. A simple traditional *Wireless Visual Sensor Network* (WVSN) is usually organized in a centralized manner and consists of: a) battery-constrained visual sensors with wireless communication capability, and b) a *Base Station* (BS) that collects the information from the sensors and decides on the resource allocation among all network nodes. Since the transmission range of a visual sensor node is limited, the recorded video sequences may need to be transmitted using fixed relay nodes until they reach the BS via multiple hops. The relay nodes utilize a *decode-and-forward* protocol. In this context, each WVSN node transmission causes interference to other transmitting nodes, which lie within its transmission range, leading to the degradation of the received video quality at the BS.

Taking into account the fact that the nodes have different resource requirements and that it is crucial to optimize communication in order to minimize energy consumption and simultaneously maintain an acceptable quality of the application requirements [2], the establishment of an efficient cross-layer method that considers all these aspects is a challenging task. Most of the works in the recent literature consider the optimization of one of the aforementioned aspects (e.g. power consumption).

Despite the QoS provisioning, a power management policy is required so that the lifetime of each battery-powered node is prolonged. At the same time, the interference among nodes that transmit simultaneously causes quality degradation, which should not be neglected by the power allocation method. Particularly, a source node's video may suffer from interference caused by other source nodes in its cluster. Furthermore, in a multihop WVSN, the relay nodes can interfere with other source and/or relay nodes. As a result, the video sequence experiences successive degradation across the multihop path to the BS. Therefore, in order to avoid such degradation, it is required to control not only the source and channel coding rates and the used transmission power of the source nodes, but also the channel coding rates and

2

the transmission power of the relay nodes. This control is performed at the BS, which collects all information from both source and relay nodes and manages the resource allocation. Nevertheless, the need to optimize both the end-to-end video quality and the power consumption has motivated us to propose a game-theoretic bi-objective approach that provides joint *Quality Enhancement and Power Control* (QEPC) for multihop WVSNs.

In the present work, we study the resource allocation problem in cooperative multihop *Direct Sequence Code Division Multiple Access* (DS-CDMA) WVSNs. Without cooperation, the nodes would simply act selfishly and greedily, thus use the highest available transmission power in order to achieve the highest possible video quality at the BS. However, this would result both in excessive power consumption and intra-cell interference, consequently leading to quality degradation and higher transmission power consumption. We consider that some of the recorded scenes are correlated in terms of their position and the levels of motion. Hence, the correlated groups of visual sensors have similar resource requirements, which allows us to accordingly cluster the visual sensors and, thus, reduce the computational complexity of the resource allocation optimization problem. Furthermore, the network resources (transmission power, source and channel coding rates) have to be optimally allocated to the source and relay nodes using a quality-aware strategy, so as to maintain the end-to-end distortion at a low level for all source nodes. Moreover, power consumption control is dictated for all WVSN nodes due to limited resources [2, 3].

Briefly, our aim is to define an effective approach for the bi-objective problem of jointly enhancing the end-to-end video quality and the total power consumption in WVSNs. To this end, in the present work, we assume that our WVSN nodes form coalitions and cooperate to establish a mutually acceptable resource allocation. We aim to satisfy both the objectives of enhanced end-to-end video quality and reduced power consumption by formulating a bi-objective utility function that acts as a pricing scheme by including both a benefit term and a cost term.

1.1. Related Work

The problem of the resource allocation in multiple network nodes for effective video streaming has been examined in many studies [4, 5, 6, 7, 8, 9, 10, 11] and various cross-layer techniques have been proposed. Some of them [4, 5, 6, 7, 8] focus on the resource allocation (e.g. bit rate or joint source and channel coding rate) for the optimization of a single objective,

3

such as throughput maximization. Other works do not take into account the resulting power consumption, like the rate-distortion scheme in [12] which adapts the transmission policy and encoding rate to channel capacity and varying correlation level of multiple scenes. Despite the effectiveness of those proposed single objective methods, they do not address the crucial issue of QEPC.

On the other hand, other studies in the recent literature [9, 10, 11, 13, 14] aim to allocate the network resources by utilizing bi-objective approaches. In [9], the joint power control and scheduling problem in wireless multihop networks is addressed with the objective of total transmission power minimization while QoS for individual sessions, in terms of payload rate and bit error rate, is guaranteed. Resource allocation schemes that enable relay node selection of each user in a cooperative network and formulate a bi-objective problem, aiming at the optimization of power consumption and throughput experienced by each node are proposed in [10]. Recognizing the fact that power control itself cannot meet the QoS requirements, a joint channel and power allocation scheme for cognitive radio networks is proposed in [11]. That scheme is designed to maximize the overall throughput, while guaranteeing the proportional fairness and power distribution among the cognitive radio users.

A joint bi-objective optimization problem was formulated in[13] for a *Orthogonal Frequency Division Multiple Access* (OFDMA) system with the decode-and-forward relaying strategy. The formulated problem was transformed in a two-stage problem in order to be solved. A similar bi-objective problem was proposed in [14] in order to solve the admission control and fair resource allocation problem in a wireless multi-user (of constant and variable bit rate) amplify-and-forward relay network. Due to its combinatorial hardness, the authors proposed its transformation into equivalent one-stage optimization problem, which can be solved with a higher computational complexity.

It is important to note that most of the proposed bi-objective problem formulations target at network-related QoS metrics optimization and not at end-to-end quality of the delivered information. Furthermore, most of these problem formulations were solved by adopting problem decomposition techniques. Instead of explicitly optimizing network-related parameters, such as bit error rate or throughput, we propose a quality-driven optimization scheme, which aims at maximizing the delivered video quality in terms of the *Peak Signal-to-Noise Ratio* (PSNR) under the network's power constraints

4

across the physical, the data link and the application layer. Moreover, we are employing the Particle Swarm Optimization algorithm that does not require modifications of the original optimization problem.

Both cooperative and non-cooperative game theoretic frameworks have been proposed for efficient resource allocation in wireless networks following either a centralized or a distributed approach. Furthermore, various game-theoretic pricing schemes regulate the resource usage through a compromise between the users' desire to optimize their own performance and the network's general need for efficient resource allocation. In this context, a Nash equilibrium based power control method that assumes a wireless relay-assisted network is proposed in [15], where the users aim to optimize their transmission rate through the power allocation process, while the relay node aims at maximizing its total rate. The users make payments to the relay according to pre-specified prices that enhance the relay's gain, as they competitively adjust their transmission powers in order to increase the received signal-to-noise ratio. Another approach [16], also utilizes the Nash equilibrium with a joint pricing scheme in a *Code Division Multiple Access* (CDMA) based network, so that both the utilities of the users and the network utility are optimized. The users' utility comprises two factors related to the achieved throughput and the energy consumption, while the network utility reflects the network energy consumption.

Many cooperative approaches utilize the *Nash Bargaining Solution* (NBS) [17] to reach a beneficial single objective resource allocation for all nodes [4, 6, 7, 8, 11, 18, 19, 13, 20]. Cooperative resource allocation schemes are a promising approach for competitive wireless environments that require proportional fairness and resource allocation among the nodes. An approach based on NBS is applied on OFDMA *Cognitive Radio* (CR) networks [11] and optimizes the overall system throughput by assigning higher priority to primary CR users, while guaranteeing a minimum throughput for both primary and secondary CR users. The problem of fair resource sharing between two selfish nodes in cooperative relay networks was considered and solved by using NBS in [20]. An interesting two-stage approach that utilizes NBS to ensure fairness in the subcarrier and power allocation problem in a relayed uplink OFDMA system is proposed in [13]. Another work that formulates Nash bargaining assigns subcarriers, transmission powers and transmit precoders to the nodes of a multiple-input and multiple-output OFDMA system [19]. Furthermore, a bi-objective NBS-based framework was applied to allocate bandwidth for elastic services in high-speed networks with fairness and in a

5

distributed manner, while maximizing the network revenue [21]. The previous work [4] was exclusively aiming at the video quality enhancement over a multihop WVSN. An extension of this work was presented in [22], where the aggregation of video quality and transmission power was employed. The present work moves beyond previous work by providing a novel problem formulation based on cooperative Game Theory and by providing enhanced fairness in the resource allocation.

Fairness in allocation problems is an issue that has been extensively studied through the years in many areas, notably in social sciences, welfare economics, and engineering [23]. However, due to the subjective interpretations of the notion of fairness, the different characteristics of allocation problems should be considered. In our case, for the evaluation of resource allocation schemes for video transmission we need a metric that expresses both the notion of fairness considering the unique video characteristics. Several approaches have been performed, which however require the utilitarian allocation (i.e. the criterion that maximizes the network utility) as a reference resource allocation scheme [24, 25, 23], or the Kalai-Smorodinsky bargaining solution as in [26].

1.2. Contribution of this paper and Structure

Related work motivated us to propose a pricing scheme that is based on cooperative game theory, and particularly on the NBS. NBS has the advantage of satisfying sets of axioms that a fairness scheme should ideally satisfy [23, 27]. We employ a bi-objective utility function that consists of a quality-related benefit term and a power-related cost term. These two terms effectively adjust the transmission power levels and at the same time result in enhanced QoS (in terms of end-to-end video quality). To the best of our knowledge, our proposed NBS-based pricing scheme has not been considered so far for similar resource allocation problems in the literature. Overall, this study moves beyond the state-of-the-art baseline by bringing the following contributions.

(i) *Bi-objective Cross-layer Problem Formulation based on NBS:* Many video transmission applications require the assignment of resources by taking into account the multi-layer structure of such networks. On the one hand, regarding the physical layer, the power consumption has to be controlled in order to prolong the WVSN lifespan and simultaneously reduce the interference among the transmitted signals. On the

6

other hand, as far as the application layer is concerned, the distortion of the delivered video sequences has to be minimized. In this cross-layer problem formulation, the allocated resources are the transmission power of the source and the relay nodes, the source coding rate at the application layer of the source nodes, and the channel coding rate at the data link layer of both the source and relay nodes. In order to solve this problem we propose to employ a pricing scheme that is based on cooperative game theory, and particularly on the NBS. In this solution, the employed bi-objective utility function consists of a *quality-related* term and a *payment* term that adjusts the transmission power levels and enables the mediation between the nodes' demands for high quality and the minimization of the power consumption.

(ii) *Proposing a Fairness metric of the resulting Video Quality:* For the assessment of the resulting end-to-end video quality, we propose a fairness metric that computes the distance of the achieved end-to-end video quality from the maximum possible video quality for each node (which could be achieved in an error-free transmission) with no reference to other resource allocation schemes and provides an overall assessment of the fairness of the resulting video quality in the network.

(iii) *Investigating the Video Quality-Power Consumption and Fairness-Power Consumption Tradeoffs:* The utility function that is employed by the proposed NBS is formulated so that it provides results on the video quality and transmission power consumption tradeoff. We study this tradeoff which leads us to significant results related to the consumed power and the video quality gain. Moreover, since in this multi-access system the resource allocation has an immediate effect on all nodes, a study on the fairness among nodes is required. Thus, we investigate the resulting fairness versus the transmission power consumption on the WVSN.

The remainder of the paper is organized as follows. Section 2 describes the considered system model. The QEPC problem formulation and its constraints are detailed in Section 3, while the NBS-based optimization criteria and the employed optimization algorithm are detailed in Section 4. The fairness metric is introduced in Section 5. The experimental results are presented in Section 6. Finally, Section 7 concludes the paper.

7

Table 1: Notations and Parameters of the System Model.

Notation	Description
(α_k, β_k)	Rate-distortion model parameters of a source node k.
(γ, δ)	Weights of the QEPC tradeoff.
$\rho_{h,n}$	Bit error probability for node n at the h-th hop.
ρ_n	End-to-end bit error probability for node n.
ϕ	Fairness index.
$k = 1, 2, \ldots, K$	Index for source nodes.
$m = 1, 2, \ldots, M$	Index for relay nodes.
$n = 1, 2, \ldots, N$	Index for network nodes
$j = 1, 2, \ldots, |\mathbf{J}|$	Index for interfering nodes at hop h.
$E\{D_{\mathrm{s+c},k}\}$	Expected distortion for source node k.
$\dfrac{E_n}{I_0 + N_0}$	Energy-per-bit to MAI and noise ratio for node n.
L	Spreading Code Length.
$PSNR_k$	Peak signal-to-Noise ratio for source node k.
$R_{\mathrm{c},k}^{\mathrm{S}}$	Channel coding rate for source node k.
$R_{\mathrm{c},m}^{\mathrm{R}}$	Channel coding rate for relay node m.
$R_y \mid y \in \{k, m, n\}$	Total transmission bit rate.(with $N = K + M$).
S_k^{S}	Transmission power of source node k.
S_m^{R}	Transmission power of relay node m.
P_k^{S}	Received power from source node k.
P_m^{R}	Received power from relay node m.
$R_{\mathrm{s},k}$	Source coding rate for source node k.
W	Channel bandwidth.

2. Description of the Considered System Model

In this section, we describe the considered model of our system. In order to enhance the reader's convenience, Table 1 summarizes the frequently used notations and parameters of our system.

2.1. DS-CDMA based System Architecture

We consider a DS-CDMA based network, where each node is associated with a spreading sequence of length L. Furthermore, *Binary Phase Shift*

8

Keying (BPSK) is used as the modulation method. Let N be the number of nodes in a synchronous single-path BPSK channel, and A_n, $b_n(i)$, $\mathbf{s}_n$, $\mathbf{u}_n$ the amplitude, symbol stream, spreading code and noise of node n respectively. For the i-th bit, the received signal can be expressed as:

$$\mathbf{r}(i) = \sqrt{q_1}\, b_1(i)\, \mathbf{s}_1 + \sum_{n=2}^{N} \sqrt{q_n}\, b_n(i)\, \mathbf{s}_n + \mathbf{u}_n \,, \qquad (1)$$

with $n = 1, 2, \ldots, N$, $i = 1, 2, \ldots, L$ and q is the received normalized power assigned per bit i. The receiver has knowledge of the spreading codes of all nodes and uses a bank of matched filters to filter out the other nodes' signals. We assume the worst-case scenario where interference is decoded as noise. The received power of a transmitting node n (in W) at the receiver is

$$P_n = E_n R_n \,, \qquad (2)$$

where E_n is the energy-per-bit and R_n the total transmission bit rate for source and channel coding in bits/sec, which is defined as:

$$R_n = \frac{R_{\mathrm{s},n}}{R_{\mathrm{c},n}} \,, \qquad (3)$$

where $R_{\mathrm{s},n}$ is the source coding rate in bits/sec and the dimensionless number $R_{\mathrm{c},n}$ is the channel coding rate. If we assume that the total transmission bit rate is constant, then a node that transmits with a lower source coding rate is able to use more bits for the channel coding. It can transmit with lower power and, as a consequence, cause less interference to other nodes' transmissions.

We assume that the BS (receiver) is out of the transmission range of the source nodes, thus relay nodes are required to forward the video data to the BS. Every source node sends its video data to the corresponding relay node of the cluster. Then, the relay node forwards the video data of all source nodes of the cluster to another relay node or to the BS. Figure 1 depicts such an example of a WVSN that comprises source nodes organized in clusters according to their location. The transmission routes are predetermined based on the location of the WVSN nodes and the source nodes transmit the recorded videos to the BS via multiple hops. The video data from the source nodes of Cluster 1 reach the BS after three hops through Relay Node 1 and Relay Node 3. The shadowed boxes show the set of interfering nodes per hop for the source nodes of Cluster 1. Particularly, in the first hop the

9

interference is caused by the source nodes within a cluster. In the second hop the nodes from Cluster 3 cause interference to the transmitted signal, and at last Relay Node 2 causes interference in the last hop. So, we denote with $\mathbf{J}$ the set that consists of the interfering nodes for each hop h, and it is assumed that $|\mathbf{J}| \leq N$, where $|.|$ is the cardinality of a set. As in the previous example, we assume that interference exists on each link across the path to the BS from nodes that are in the effective transmission range. Similar to other approaches [28], we model interference as *Additive White Gaussian Noise* (AWGN). The energy-per-bit to *Multiple Access Interference* (MAI) and noise ratio is different in each link, depending on the nodes causing interference to the considered node n and can be expressed for the h-th hop of a path as follows:

$$\frac{E_n}{I_0 + N_0} = \frac{\dfrac{P_n}{R_n}}{\displaystyle\sum_{j=1, j\neq n}^{|\mathbf{J}|} \dfrac{P_j}{W} + N_0},\tag{4}$$

where $I_0/2$ is the two sided noise power spectral density due to MAI, $N_0/2$ is
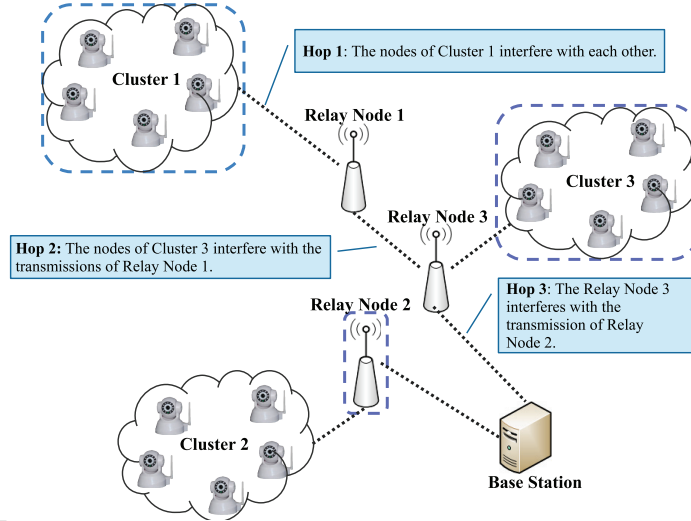

Figure 1: Example of a multihop WVSN. The video data from the source nodes of Cluster 1 reach the Base Station after two hops through Relay Node 1 and Relay Node 3. The outlined boxes show the set of interfering nodes $\mathbf{J}$ per hop for the source nodes of Cluster 1.

10

the two sided noise power spectral density of the background noise in W/Hz, W is the total bandwidth in Hz and P_j is the received power from node $j \in \mathbf{J}$ that causes interference to node n.

Depending on the terrain profile, different radio propagation models could be employed to calculate the required transmitted power of a node. For the present work, we assume clear line of sight and, therefore, employ a mixed scenario that consists of two propagation models; the *Free Space* (FS) and the *Two Ray Ground Reflection* (TRGR) models [29]. Particularly, for a given received power P_n at a distance y from a node n, the required transmitted power S_n is calculated based on the FS model when the communication distance is under a threshold (which is called the crossover distance y_0), otherwise it is calculated based on the TRGR model, i.e.

$$
P_n(y) = \begin{cases} S_n \dfrac{G_t G_r \lambda^2}{(4\pi)^2 y^2 l} & \text{if } y \leq y_0 \quad \text{(FS Model)} \\[3mm] S_n \dfrac{G_t G_r h_t^2 h_r^2}{y^4 l} & \text{if } y > y_0 \quad \text{(TRGR Model)} \end{cases}
\tag{5}
$$

where y is the communication distance, $l \geq 1$ is the system loss factor not related to propagation, λ the wavelength of the carrier signal, (G_t, G_r) and (h_t, h_r) are the antenna gain and height for the transmitter and the receiver, respectively. The cross-over distance y_0 is calculated by equating the expressions for the FS and the TRGR model, i.e. $y_0 = \dfrac{4\pi h_r h_t \sqrt{l}}{\lambda}$. The used model takes advantage of the better accuracy of the TRGR model for long distances while it avoids its poor performance for short distances.

2.2. Channel Coding

For the channel coding of the transmitted signal *Forward Error Correction* (FEC) is employed. In this work, we use the *Rate Compatible Punctured Convolutional codes* (RCPC), which map information to code bits sequentially with an encoding process that involves convolution of the information data with a generator sequence. However, other error correction codes could be used instead.

The end-to-end bit error probability ρ_n for a node n in a multihop transmission of the video across an H-hop path is [30]:

$$
\rho_n = 1 - \prod_{h=1}^{H} (1 - \rho_{h,n}) ,
\tag{6}
$$

11

where $\rho_{h,n}$ is the bit error probability at hop h for the node n. When we refer to bit error probability at hop h, we mean the bit error probability for the transmission over the link that is counted as hop h. The different sources of interference are considered at each hop, i.e. at each video stream transmission over a link. [2]

Furthermore, the Viterbi upper bound for the bit error probability $\rho_{h,n}$ can be given by:

$$\rho_{h,n} \leq \frac{1}{T} \sum_{d=d_{\text{free}}}^{\infty} c_d \rho_d \tag{7}$$

where T is the period of code, ρ_d is the pairwise error probability in choosing between two paths of mutual Hamming distance d, d_{free} is the minimum Hamming distance between two different coded sequences (free distance of the code) and c_d is the information error weight [31]. Considering an AWGN channel with BPSK modulation, the pairwise error probability from Eq. (7) is given by:

$$\rho_d = \text{erfc} \left(\sqrt{d\, R_c \frac{E_n}{I_0 + N_0}} \right) \tag{8}$$

where R_c is the channel coding rate and erfc(.) is the complementary error function given by:

$$\text{erfc}(z) = \left(2 \int_z^{\infty} \exp(-t^2) dt \right) / \sqrt{\pi}. \tag{9}$$

2.3. Source Coding and Video Distortion Estimation

For the compression of the video sequences used for transmission, the H.264/AVC video coding standard is utilized. H.264/AVC allows to maintain the same level of video quality as previous codecs at a significantly lower bit rate. The H.264/AVC standard covers two layers in order to offer a network-friendly design to both real-time and non-conversational applications. The first is the *Video Coding Layer* (VCL), which represents the video content as coded information achieving a high level of compression. The other is the *Network Abstraction Layer* (NAL), which formats the VCL data and provides

---

[2]This becomes clear from Eq. (8), where the pairwise error probability depends on the energy-per-bit to MAI and noise ratio per hop.

12

information about the transmission of the encoded data over the network [32]. The VCL of H.264/AVC utilizes block-based hybrid video coding.

Due to random errors that occur during the multihop transmission, the video distortion $D_{s+c,k}$ of a source node k is a random variable. Thus, we calculate the value of the expected distortion $E\{D_{s+c,k}\}$. In order to calculate the expected distortion as a function of the bit error probabilities after channel decoding, we use the *Universal Rate-Distortion Characteristics* (URDCs) [33]. By definition, the URDC model provides an estimation of the expected video distortion due to compression and channel errors given a bit error probability for a specific source coding rate. This means that URDCs take into consideration the error propagation in the video stream in a macroscopic manner.

Owing to Eq. (6), the expected distortion due to lossy compression and channel errors can be derived by the model for the URDC of each source node k used in [6, 8, 34]:

$$E\{D_{s+c,k}\} = \alpha_k \left[\log_{10} \left(\frac{1}{1 - \prod\limits_{h=1}^{H} (1 - \rho_{h,k})} \right) \right]^{-\beta_k}, \qquad (10)$$

where parameters α_k and β_k are positive numbers that depend on the motion level of the transmitted video sequence and the source coding rate and may vary in time. Values of α_k for high motion video sequences are generally greater than those for low motion video sequences. These parameters are determined using mean square optimization from a few $(E\{D_{s+c,k}\}, \rho_k)$ pairs.

For the estimation of $E[D_{s+c,k}]$ at the encoder, the *Recursive Optimal per-Pixel Estimate* (ROPE) algorithm [35] is used. The ROPE algorithm recursively calculates in real time the first and second moments of the decoder reconstruction of each pixel, while it accurately takes into account all relevant factors that cause video distortion, namely quantization errors, packet losses, error propagation and error concealment. The algorithm for all this process is detailed in [36]. Since parameters α_k, β_k depend on the varying motion levels of the recorded scenes, they need to be recalculated when the motion changes significantly. For small motion variations, parameters α_k, β_k values change slightly, thus the nodes may continue using the same WVSN resources. Besides, in such cases a resource reallocation would slightly affect the end-to-end quality and the total transmission power consumption. A continuous recalculation (e.g. per frame) of parameters α_k, β_k would burden

13

our system with a high computational cost. Hence, we propose a periodic calculation of these parameters. If the recalculation of parameters α_k, β_k reveals a significant change of their values, then we transmit them to the BS. For transferring these parameters from each source node to the BS, we propose a low-cost in-band solution. Note that only a few bytes are enough for representing both α_k and β_k, therefore this information can be piggybacked on the header of data packets. In this way, we minimize the cost since we do not burden the wireless medium with extra packets.

From Eqs. (3)-(10), it follows that $E\{D_{\mathrm{s+c},k}\}$ of the video of source node k is a function of the source coding rate $R_{\mathrm{s},k}$, the channel coding rate $R_{\mathrm{c},k}^{\mathrm{S}}$, the received power P_k^{S} and the channel coding rate $R_{\mathrm{c},m}^{\mathrm{R}}$ and the received power P_m^{R} of each relay node m that retransmits the video of k across its path to the BS. Moreover, due to interference (Eq. (4)), the expected video distortion also depends on the received powers from the interfering nodes per hop.

3. Joint Quality Enhancement and Power Control: Problem Formulation

In this section, we describe the constraints and the formulation of the problem of the joint QEPC in a multihop DS-CDMA WVSN.

3.1. Constraints

Regarding the system which is described in Section 2, we make assumptions that impose the following constraints on the admissible values of source and channel coding rates, transmission bitrates and transmission powers of the considered WVSN's source and relay nodes.

Letting $\mathcal{A}$ be the discrete set of $|\mathcal{A}|$ valid source and channel coding rate pairs for each source node k and $\mathcal{B}$ the discrete set of $|\mathcal{B}|$ channel coding rate choices for each relay node m, we set that our resource allocation scheme is subject to:

$$(R_{\mathrm{s},k}, R_{\mathrm{c},k}^{\mathrm{S}}) \in \mathcal{A} = \{(R_{\mathrm{s}}^1, R_{\mathrm{c}}^{\mathrm{S},1}), \ldots, (R_{\mathrm{s}}^{|\mathcal{A}|}, R_{\mathrm{c}}^{\mathrm{S},|\mathcal{A}|})\}, \tag{11}$$

$$\frac{R_{\mathrm{s}}^1}{R_{\mathrm{c}}^{\mathrm{S},1}} = \frac{R_{\mathrm{s}}^2}{R_{\mathrm{c}}^{\mathrm{S},2}} = \ldots = \frac{R_{\mathrm{s}}^{|\mathcal{A}|}}{R_{\mathrm{c}}^{\mathrm{S},|\mathcal{A}|}} = R_k \ \forall k\,, \tag{12}$$

$$R_{\mathrm{c},m}^{\mathrm{R}} \in \mathcal{B} = \{R_{\mathrm{c}}^{\mathrm{R},1}, \ldots, R_{\mathrm{c}}^{\mathrm{R},|\mathcal{B}|}\}\,. \tag{13}$$

14

It is also important to take into consideration that each relay node m needs to use a sufficient bit rate for the simultaneous forwarding of all received video data. This is related to the source coding rate of the transmitting source nodes. Since the relay nodes channel decode-and-forward the received video data, it is required to have enough bits for both the video data and the redundancy bits of the channel coding. Hence, the transmission bit rate of a relay m is

$$R_m \geq \frac{\sum\limits_{z \in \mathbf{Z}} R_{\mathrm{s},z}}{R_{\mathrm{c},m}^{\mathrm{R}}} , \tag{14}$$

where $\mathbf{Z}$ is the set of the source nodes that use relay node m for their data forwarding and $R_{\mathrm{c},m}^{\mathrm{R}}$ is the channel coding rate for relay node m.

A last constraint imposed on the system concerns the admissible transmission power for the source and relay nodes. Particularly, both types of WVSN nodes have a lower and an upper transmission power bound, i.e. $S_k^{\mathrm{S}} \in \left[S_{\min}^{\mathrm{S}}, S_{\max}^{\mathrm{S}} \right]$ and $S_m^{\mathrm{R}} \in \left[S_{\min}^{\mathrm{R}}, S_{\max}^{\mathrm{R}} \right]$. Obviously, using Eq. (5), this constraint is transformed into a constraint on the received power levels.

3.2. Problem Formulation

In this context, we propose a technique that offers a prioritized enhancement of the end-to-end video quality and manages the transmission power allocation according to the importance of the video sequences of the WVSN source nodes. It aims at optimally allocating the source and channel coding rates and the transmitted powers among the source nodes of a WVSN and at the same time the necessary channel coding rates and transmitted powers to the relay nodes. For the assignment of the available resources, a compromise between the power consumption and the distortion of the delivered video sequences has to be established. Therefore, we define the bi-objective QEPC problem that actually minimizes a function of both the expected distortions of the received videos and the received powers. Then, based on the employed radio propagation models (see Eq. (5)) we compute the transmission powers.

We first define the following vectors for the received powers, source and channel coding rates of K source nodes and M relay nodes, respectively:

$P = (P_1^{\mathrm{S}}, P_2^{\mathrm{S}}, \dots, P_K^{\mathrm{S}}, P_1^{R}, P_2^{R}, \dots, P_M^{\mathrm{R}})^{\top};$
$R_{\mathrm{s}} = (R_{\mathrm{s},1}, R_{\mathrm{s},2}, \dots, R_{\mathrm{s},K})^{\top};$
$R_{\mathrm{c}} = (R_{\mathrm{c},1}^{\mathrm{S}}, R_{\mathrm{c},2}^{\mathrm{S}}, \dots, R_{\mathrm{c},K}^{\mathrm{S}}, R_{\mathrm{c},1}^{\mathrm{R}}, R_{\mathrm{c},2}^{\mathrm{R}}, \dots, R_{\mathrm{c},M}^{\mathrm{R}})^{\top}.$

15

Our proposed method determines for each source node k the source coding rate $R_{s,k}$, the channel coding rate $R_{c,k}^S$ and the received power P_k^S and for each relay node m the channel coding rate $R_{c,m}^R$ and the received power P_m^R, so that a function $\mathcal{F}(.)$ of the overall end-to-end expected video distortion $E\{D_{s+c,k}\}$ for each source node k and the received power P from both the source and relay nodes is minimized, i.e.

$$(R_s^*, R_c^*, P^*) = \arg \min_{R_s, R_c, P} \mathcal{F}(E\{D_{s+c,1}\}, \ldots, E\{D_{s+c,K}\}, P)$$

subject to the constraints described in Section 3.1. The type of the function $\mathcal{F}(.)$ is different for each one of the deployed optimization criteria, which we delineate in Section 4.

For conveying the results of the optimization from the BS to the source and relay nodes, we propose an out-of-band solution, i.e. the use of a dedicated channel (e.g. a different spreading code). This information to be conveyed sums up to a few bytes, therefore the BS should include it in a single message and broadcast that message to the nodes. The use of a dedicated channel secures the timely delivery of the information from the BS to the nodes, while broadcasting a single message, each time the optimization process is performed, minimizes the bandwidth requirements.

4. Bi-objective Optimization Criteria

The described QEPC problem is solved using the NBS with equal or different bargaining powers, formulating two bi-objective criteria. The first criterion employs the NBS with equal bargaining powers while the second criterion uses different motion-related bargaining powers.

4.1. Bi-objective Utility Function

Based on Game Theory, and particularly on the NBS, a bargaining game is organized for the resource allocation among the WVSN nodes. The nodes of a DS-CDMA based multihop WVSN interfere with each other, as they all transmit simultaneously. Each node tries to increase its transmitted power, aiming at a better quality for its video, but this can also lead to the degradation of the quality of the other nodes' videos. It is therefore essential that cooperation exists among the nodes in the multihop path to the BS. In this way, the resources are allocated so that a good quality, namely a good PSNR,

is achieved for all nodes. For the arising bargaining problem, a measure of satisfaction of the demands of a source node k is the *utility function*.

In the present paper, it is proposed to be formulated in a way that both the aspiration of node k to increase its benefit in terms of the video quality and its willingness to pay for the cost related to transmission power of all relay nodes employed for the video data forwarding of node k are demonstrated:

$$U_k = \gamma PSNR_k - \delta(P_k^{\mathrm{S}} + \sum_{y=1}^{Y} P_y^{\mathrm{R}}), \qquad (15)$$

where $y = 1, 2, \ldots, Y$ is a counter for the relay nodes that a source node k uses for transmission, parameters γ and δ are non-negative weights with $\gamma + \delta = 1$, and $PSNR_k$ expresses the video quality in dB per source node k. The complementary weights show the relative importance of the different objectives. Moreover, by definition the convex hull of two objectives is their convex combination. Thus, the convex combination of the two objectives covers all points in the convex hull. PSNR is defined as a function of $E\{D_{\mathrm{s+c},k}\}$, i.e. $PSNR_k = 10 \log_{10} \dfrac{255^2}{E\{D_{\mathrm{s+c},k}\}}$. Thus, it depends on the source and channel coding rate of the source node k, and the received power from all nodes (because the received power plays important role during the transmission from the source node k to the BS through all relay nodes that are employed for the video data forwarding of source node k). The defined utility function of Eq. (15) depends on the same parameters, as well. The values of γ and δ can be tweaked so that the tradeoff between the resulting PSNR and the used transmission powers is regulated.

The minimum utility the players expect to receive if negotiations break down is expressed by the *disagreement point* $d = (d_1, \ldots, d_K)^{\top}$. Theoretically, the utility of each player after the cooperation is not allowed to be smaller than it would be if the player did not join the bargaining game (as also inferred by the feasibility axiom provided in Section 4.2) [37]. This means that every cooperating player should either have a gain or remain with the same utility it had before the cooperation. In this particular bargaining game, the disagreement point $d \in \mathbf{U}$ expresses both the minimum acceptable quality (in terms of PSNR) for each video and the maximum allowed transmission power for both the source and its relay nodes, i.e.

$$d_k = \gamma PSNR_{\mathrm{min},k} - \delta(P_{\mathrm{max}}^{\mathrm{S}} + Y \ P_{\mathrm{max}}^{\mathrm{R}}) , \qquad (16)$$

17

where Y is the total number of the relay nodes that a source node k uses for transmission. It is important to notice that both the $PSNR_{\min,k}$ and the $P_{\max}^{\mathrm{S}}$, $P_{\max}^{\mathrm{R}}$ values are specified by the QoS requirements of a certain application.

4.2. Nash Bargaining Solution and related criteria

Based on the NBS, we define the bargaining game deployed in our resource allocation scheme as a pair $(\mathbf{U}, d)$, where the *feasible set* $\mathbf{U} \subset \mathbb{R}^K$ is the set of all possible vectors $U = (U_1, U_2, \ldots, U_K)^\top$. Each one of the possible vectors U results from different combinations of the vectors of the received power from the K source nodes and the M relay nodes, the source coding rate of the source nodes and the channel coding rate for all nodes and represents the feasible payoffs (resource allocations) of the players (source nodes). It is mandatory that this set is closed, bounded above, comprehensive, and that free disposal is allowed [38].

The NBS can be written as a function $\mathcal{G}(.)$ of $\mathbf{U}$ and d, i.e. $\mathcal{G}(\mathbf{U}, d) \in \mathbf{U}$, and satisfies three axioms. These axioms guarantee that the solution is Pareto optimal, invariant to affine transformations, and independent from irrelevant alternatives [37]:

(i) $\mathcal{G}(\mathbf{U}, d) \geq d$ and $y > \mathcal{G}(\mathbf{U}, d) \Rightarrow y \notin \mathbf{U}$.

(ii) Given any strictly increasing affine transformation $\tau(.)$, $\mathcal{G}(\tau(\mathbf{U}), \tau(d)) = \tau(\mathcal{G}(\mathbf{U}, d))$.

(iii) If $d \in \mathbf{Y} \subseteq \mathbf{U}$, then $\mathcal{G}(\mathbf{U}, d) \in \mathbf{Y} \Rightarrow \mathcal{G}(\mathbf{Y}, d) = \mathcal{G}(\mathbf{U}, d)$.

The NBS of this multi-player cooperative bargaining game can be found by maximizing the Nash Product:

$$\mathcal{G}(\mathbf{U}, d) = \arg \max_U \prod_{k=1}^{K} (U_k - d_k)^{b_k} \tag{17}$$

subject to the constraints: $(U_k - d_k) > 0$, $\sum_{k=1}^{K} b_k = 1$ and those described in Section 3.1.

The value b_k refers to the *bargaining power* of a source node k. The bargaining power indicates the advantage the node has in the bargaining game. It is assigned in accordance with the rules of the bargaining game. A node with a higher bargaining power is favored by the rules of the bargaining game compared to a node with a lower bargaining power.

18

4.2.1. NBS-based Criteria

Similar to [8], we consider two different NBS-based criteria according to the different definition of the bargaining powers of the nodes as follows.

(i) *Using equal bargaining powers* (e.NBS): This criterion assumes that all bargaining powers are assigned the same value, i.e.

$$b_k = \frac{1}{K} \; . \tag{18}$$

(ii) *Using motion-related bargaining powers* (w.NBS): This criterion assigns to each node a different bargaining power which is motion-related according to parameters α_k of Eq. (10), i.e.

$$b_k = \frac{\alpha_k}{\sum_{i=1}^{K} \alpha_i}, \quad \text{with} \quad i = 1, 2, \ldots, K \; . \tag{19}$$

4.3. Optimization Algorithm

In the proposed scheme, the received and transmitted powers are assumed to take continuous values within a specified range, whereas the source and channel coding rates take discrete values. Thus, the formulated optimization problems are mixed integer problems. For this reason, a stochastic optimization technique is selected, namely *Particle Swarm Optimization* (PSO) [39, 40].

PSO is an efficient, adjustable, and easily implementable population-based algorithm for black-box optimization. It was inspired by the social dynamics observed in hierarchically organized societies. Essentially, PSO mimics the behavior of a fixed-size population, called a *swarm*. It consists of a number of search agents, called the *particles*, which iteratively probe the search space in order to find solutions for the problem at hand.

Each particle has a memory where it stores the best position it has ever visited during its search, i.e., the position with the lowest function value (in minimization problems). Also, the particles exchange information among them, based on abstract communication schemes. These schemes can be represented by graphs where nodes correspond to particles and interconnections represent communication links among them. These schemes are also called neighborhood topologies, and they can have crucial impact on the information flow within the swarm.

19

4.3.1. Motivating the use of PSO

The PSO algorithm is one of the most popular population-based, stochastic optimization algorithms. Its efficiency has been shown in a plethora of engineering problems, along with its superiority against other (deterministic and stochastic) global optimization methods (e.g. see applications in [39, 41, 42, 43]). Moreover, PSO is accompanied by strong theoretical results regarding its stability, convergence properties, and parameter settings (see [40, 44, 45, 46, 47]). Recently, PSO was used in relevant applications with remarkable success [18, 36, 48]. In fact in [18], it was shown to be more efficient than deterministic approaches that are typically used in such problems.

In various multi-objective engineering problems, it is common to apply normalization of the objectives prior to the mathematical solution of the problem. However, when it comes to metaheuristic optimization algorithms, the merit of normalization is mostly related to the interpretation of the solutions rather than the solver itself. PSO has been applied in a plethora of problems without normalizing the objective functions (see [49]).

All these reasons, along with the high nonlinearity of the involved objective functions in our problem as well as PSO's tolerance in noisy environments that are usually met in real-world applications, were our main incentives for the use of the specific algorithm.

4.3.2. Using a rough estimation for swarm initialization

In the present work, we use PSO with a different swarm initialization scheme based on a *Rough Estimation* (PSO-RE). This initialization scheme, introduced in [36], offers the advantage of faster convergence compared to PSO. Let $\mathcal{Q} = \{x_1, x_2, \ldots, x_{|\mathcal{Q}|}\}$ be a swarm consisting of $|\mathcal{Q}|$ particles, where $|.|$ denotes the cardinality of a set. Each particle is defined as a multi-dimensional vector, $x_i \in X$, $i = 1, 2..$, where X is the search space. In our problem, x_i consists of resources that need to be allocated, namely the parameters P_k^{S}, $R_{\mathrm{s},k}$ and $R_{\mathrm{c},k}^{\mathrm{S}}$ for each source node k and of the parameters P_m^{R} and $R_{\mathrm{c},m}^{\mathrm{R}}$ for each relay node m, as defined in Section 3.2.

For the swarm initialization, according to PSO-RE, we use a rough first estimation of the resource allocation, based on the expected received power of each node as proposed in [36]. Particularly, for the source nodes we use the following equation:

$$\hat{P}_k^{\mathrm{S}} = \frac{\alpha_k}{\min(\alpha)} \, P_{\min}^{\mathrm{S}}, \tag{20}$$

20

where $\alpha = (\alpha_1, \alpha_2, \ldots, \alpha_K)^\top$ is the vector of the α_k values for each source node k, and $\min(\alpha)$ is the minimum element of vector α. We use the same equation for the rough estimation of the expected received power $\hat{P}_m^{\mathrm{R}}$ of each relay node, since we observed from the conducted experiments and our previous work [4] that the relay nodes require a power level proportional to the power level of the cluster nodes in their reception range. For half of the particles of the swarm, we initialize the components that correspond to the expected received power as computed by Eq. (20). For the integer components of the swarm, namely the source and channel coding rates, we randomly assign to them one of the available values. The other half of the swarm is randomly initialized in the search space, as performed in the traditional PSO algorithm.

Moreover, letting v_i be the corresponding velocity, $p_i \in \mathcal{Q}$ the best position of the i-th particle, and t the current iteration of the algorithm, then the velocity and current position of x_i are updated according to the equations [43]:

$$
\begin{aligned}
v_i(t+1) &= \chi\Big[v_i(t) + c_1\mathcal{R}_1\big(p_i(t) - x_i(t)\big) + c_2\mathcal{R}_2\big(p_{g_i}(t) - x_i(t)\big)\Big], & (21) \\
x_i(t+1) &= x_i(t) + v_i(t+1), & (22)
\end{aligned}
$$

where χ is a parameter called the *constriction coefficient*, c_1, c_2 are positive acceleration parameters called *cognitive* and *social* parameter, respectively, and $\mathcal{R}_1$, $\mathcal{R}_2$ are vectors with components uniformly distributed in the range $[0, 1]$. All vector operations in Eqs. (21) and (22) are performed componentwise. Also, the best position p_{g_i} of each particle i is updated as soon as it discovers a better one. Clerc and Kennedy [43] proposed parameter values that promote convergence of the algorithm towards the most promising solutions in the search space. Based on this study, the default set of parameters is defined as $\chi = 0.729$, $c_1 = c_2 = 2.05$.

5. Fairness of the Resource Allocation based on the Delivered Video Quality

In video transmission systems, the end-to-end video distortion is a result of compression errors and transmission errors. Thus, the overall distortion is the superposition of these two types of distortion. Due to the different rate-distortion characteristics, each video has different average MSE value after the video compression for the different source coding rates. If we considered

21

that the transmission of a video is error-free, then its average MSE value at the receiver would be equal to its MSE value after video encoding. This MSE value in terms of PSNR is the maximum quality $PSNR_{\max}$, which could be ideally achieved in an error-free transmission.

We propose to define the fairness of the resulting resource allocation with regard to the distance of the resulting PSNR values from their corresponding maximum video quality values $PSNR_{\max}$. We assume that $PSNR_{\max,k}$ is utopian. We consider as fair resource allocation the one that achieves the same video quality distance for all nodes from its utopian quality value. This consideration is expected to provide a better assessment of the fairness of the resource allocation among the WVSN nodes. For this reason, based on a quantitative measure that was first proposed for operation systems resource allocation [50] (and has been used before in similar resource allocation problems [10, 11] for different notions), we define the *fairness index* ϕ, as follows:

$$\phi = \frac{\left(\sum\limits_{k=1}^{K} PSNR_{\max,k} - PSNR_k \right)^2}{K \sum\limits_{k=1}^{K} (PSNR_{\max,k} - PSNR_k)^2} , \qquad (23)$$

where $PSNR_k$ reflects the end-to-end video quality of source node k and $PSNR_k < PSNR_{\max,k}$. ϕ assumes values in $(0, 1]$ and is equal to one when all achieved PSNR values are equally distant from their utopian quality values. On the contrary, when the difference values $PSNR_{\max,k} - PSNR_k$ of the different source nodes are dispersed, ϕ reduces.

6. Experimental Results

In this section, we evaluate the performance of the proposed method, which is tested in two topologies with different network configurations.

6.1. Experimental Settings

6.1.1. Considered WVSN scenarios and topologies

For the experimental settings, we assume that neighboring visual sensors monitor the same area. Due to this assumption, the neighboring nodes are organized with respect to their location in clusters and transmit video sequences of the same motion level. Thus, the (α_k, β_k) parameters of nodes in

22

Table 2: Key Parameters and Values for the Experiments.

Description	Notation	Topology I	Topology II
Number of source nodes	K	20	15
Number of clusters	C	4	3
Number of relay nodes	M	4	2
Transmission bit rate for relay nodes (kbps)	R_m	$\forall m : 480$	$m = 1:\ 480,\ m = 2:\ 960$
Channel bandwidth (MHz)	W_{t}	5	4
Transmission power of source nodes (W)	S_k^{S}	$\forall k : [0.1, 0.5]$	$\forall k : [0.1, 0.5]$
Transmission power of relay nodes (W)	S_m^{R}	$\forall m : [0.1, 5]$	$m = 1:\ [0.1, 2.5],\ m = 2:\ [0.1, 5]$
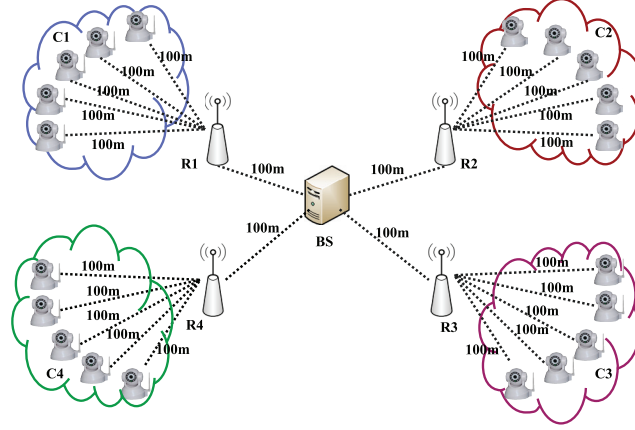
Figure 2: The first considered WVSN topology, Topology I, for the experiments.

a cluster are considered to be equal. The main parameters of the presented experiments and their values for each topology are reported in Table 2.

In order to further assess the performance of our method, several cases with different motion levels (low, medium and high) per cluster have been considered. The terms "low", "medium" and "high" motion are used for video sequences of similar motion levels with the 10-second, 15 fps, "Akiyo", "Salesman" and "Foreman" QCIF video sequences, respectively.

Topology I. In the first considered WVSN topology, which is illustrated in Fig. 2, 20 source nodes are organized in four clusters $\{C1, C2, C3, C4\}$ of the same cardinality. As the BS is out of the transmission range of the source nodes, one of the relay nodes $\{R1, R2, R3, R4\}$ is committed to each cluster in order to channel-decode-and-forward the video data to the BS. Interference
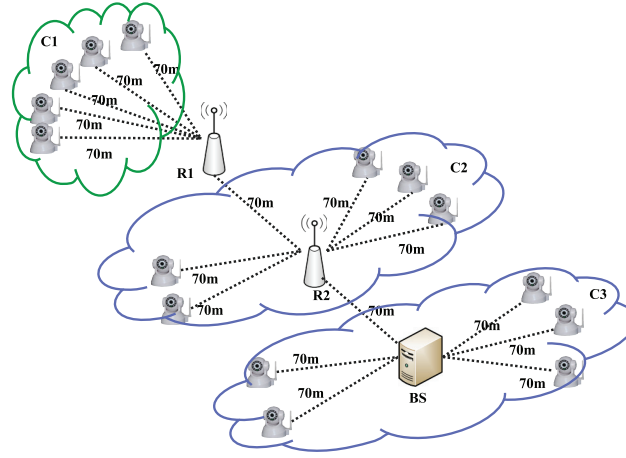
23

Figure 3: The second considered WVSN topology, Topology II, for the experiments.

exists among the nodes within a cluster as they transmit their videos to their corresponding relay node, for example for each one of the source nodes of C1 the rest source nodes of C1 cause interference in the first hop. Moreover, the four relay nodes interfere with each other when they retransmit videos to the BS. Regarding the motion level of each cluster, $C1$'s nodes transmit high motion videos while the nodes of cluster $C2$ transmit low motion videos and the nodes of clusters $C3$ and $C4$ transmit different medium motion videos.

Topology II. The second WVSN topology, Topology II, consists of 15 nodes, organized in three clusters $\{C1, C2, C3\}$, as depicted in Fig. 3. The BS is out of the transmission range of the source nodes in clusters $C1$ and $C2$, thus two relay nodes are used $\{R1, R2\}$ for the retransmission of videos of these clusters to the BS. The source nodes of cluster $C3$ directly transmit the videos to the BS. Similarly to the first topology, interference exists among the source nodes in the same cluster. The relay nodes $R1$ and $R2$ interfere with the source nodes in clusters $C2$ and $C3$, respectively. The nodes of each cluster transmit video sequences of the same motion level. In particular, the nodes of $C1$ transmit low motion level videos, the nodes of $C2$ medium motion videos and the nodes of $C3$ transmit high motion level video.

24

6.1.2. Experimental Settings and Parameters

The main parameters of the presented experiments and their values are reported in Table 2. Since our proposed method is quality-driven, we consider that the resulting video quality is at least of equal preference as the power consumption. Hence, regarding the values of (γ, δ), we consider the range $[0.50, 1.00]$ for γ and $[0.00, 0.50]$ for δ. In order to reduce the infinite number of points in these ranges, we assume that γ and δ can take values within the following sets with a step size equal to 0.01: $\gamma \in \{0.50, 0.51, \ldots, 0.99, 1.00\} \subset [0.50, 1.00]$ and $\delta \in \{0.00, 0.01, \ldots, 0.49, 0.50\} \subset [0.00, 0.50]$, so that $\gamma + \delta = 1$.

In both tested topologies, the transmission bit rate of the source nodes is 96 kbps and the transmission bit rates of the relay nodes are reported in Table 2. The minimum acceptable PSNR (a.k.a the disagreement point) is set to 24 dB. We also set $G_t = G_r = 3$ dB, $h_t = h_r = 3$ m and $N_0 = 1$ pW/Hz, while RCPC codes with mother rate 1/4 are used.

In the present formulated problem, source and channel coding rates are selected from a discrete set and are available as combinations of (R_s, R_c) for the source nodes and as single choices, R_c, for the relay nodes. Specifically, as also displayed in Table 2, we assumed the following code set and correspondences:

(i) for the source nodes: 1 for (32 kbps, 1/3), 2 for (48 kbps, 1/2) and 3 for (64 kbps, 2/3);

(ii) for the relay nodes: 1 for 1/3, 2 for 1/2 and 3 for 2/3.

Thus, our optimization problem is a mixed-integer one, since the transmission powers are continuous and the source-channel coding rate combinations are discrete (in our case they can take values 1, 2, and 3). Note that instead of 1, 2 and 3, we could use three other successive numbers (e.g. 7, 8, 9). Due to the fact that PSO particles probe the search space in the continuous range defined by its frontiers, in order to solve this mixed-integer problem, the source and channel coding rates were represented with continuous values. Taking into consideration that we have assumed the aforementioned correspondences for the valid source and channel coding rates, we have used the range $[0.6, 3.4]$ as the continuous range of this values. (If three other successive integer numbers were used for these correspondences, then this range would be different, e.g. for $\{7, 8, 9\}$ the range would be $[6.6, 9.4]$) However, these values are rounded to the nearest integer before each particle x_i objective function evaluation, namely $x_i = \lfloor x_i + 0.5 \rfloor$. For example, if we assume that for a particle the

25

source and channel coding rate value is probed in 0.875 value, then before the particle's objective function evaluation 0.875 will be rounded to 1. So, 1 will be used to evaluate the objective function value for the specific particle.

6.2. Results and Discussion

In the presented results, we compare the performance of the proposed QEPC method with the method introduced in [4], which performs resource allocation without power control ($\gamma = 1.00, \delta = 0.00$). Moreover, we compare the results of the NBS-based criteria with two aggregation criteria, EWAD and MWAD, formulated in [22] and shown in Table 3. These criteria minimize the weighted aggregation of expected distortion of source nodes and the aggregation of the received powers of source and relay nodes. They either treat all source nodes equally (EWAD criterion) or use motion-related weights in order to prioritize the quality enhancement of higher motion videos (MWAD criterion). We build our discussion around the important issues of the WVSN power consumption, its tradeoff with end-to-end video quality and the resulting fairness based on the results for Topology I. For Topology II, the proposed method has a very similar performance with analogous results, thus the same observations and conclusions are drawn.

Table 3: State-of-the-Art Criteria used for results assessment.

Name	Acronym	Formulation
Equally Weighted Aggregation of Distortion	EWAD	$\mathcal{F} = \sum\limits_{i=1}^{K} E\{D_{\mathrm{s+c},i}\} + \sum\limits_{j=1}^{K+M} P_j$
Motion-related Weighted Aggregation of Distortion	MWAD	$\mathcal{F} = \sum\limits_{i=1}^{K} w_i E\{D_{\mathrm{s+c},i}\} + \sum\limits_{j=1}^{K+M} P_j,$ with $w_i = \dfrac{\alpha_k}{\sum\limits_{i=1}^{K} \alpha_i}$

6.2.1. Allocated Source and Channel Coding Rates

Table 4 reports the resulting source and channel coding selection for each cluster from the set $\mathcal{A}$ and the channel coding selection for relay nodes from the set $\mathcal{B}$ for different values of (γ, δ). As far as the resulting channel coding rates for the relays are concerned, the highest rate has been selected in all cases for all relays, i.e. equal to 2/3. Besides this, we observe that the highest source coding rate is selected for the cluster with high amount of motion videos in almost all cases. Moreover, the motion-aware criteria w.NBS

26

Table 4: Source and Channel Coding Rates per cluster and relay for the various values of γ.

Criterion	e.NBS				w.NBS				EWAD				MWAD			
Cluster	C1	C2	C3	C4	C1	C2	C3	C4	C1	C2	C3	C4	C1	C2	C3	C4
$\gamma = 0.50$	1	2	2	2	3	1	1	1	3	2	1	2	3	1	1	2
$0.51 \leq \gamma \leq 0.53$	1	2	2	2	3	1	1	1	3	2	2	2	3	1	2	2
$0.54 \leq \gamma \leq 0.69]$	3	2	2	2	3	1	1	1	3	2	2	2	3	1	2	2
$0.70 \leq \gamma \leq 0.75$	3	2	2	2	3	1	1	2	3	2	2	2	3	1	2	2
$0.76 \leq \gamma \leq 0.83$	3	3	2	2	3	1	1	2	3	2	2	2	3	1	2	2
$0.84 \leq \gamma \leq 1.00$	3	3	2	2	3	1	2	2	3	2	2	2	3	1	2	2
Relay	R1	R2	R3	R4	R1	R2	R3	R4	R1	R2	R3	R4	R1	R2	R3	R4
$0.50 \leq \gamma \leq 1.00$	3	3	3	3	3	3	3	3	3	3	3	3	3	3	3	3

and MWAD use lower source coding rates for the nodes of low and medium amount of motion, compared to the other two criteria. This, in combination with the fact that video sequences of low amount of motion are more robust to errors, means that lower transmission power is required for those nodes.

6.2.2. Transmission Power Consumption

The allocated transmission power for the source nodes in a cluster and their respective relay nodes are plotted in Fig. 4 and Fig. 5, respectively. A close inspection of the figures reveals that the allocated transmission powers for each cluster and for each relay are in line with the motion levels of the recorded scenes. The effect of power control is witnessed intensely in Fig. 4, where we notice that for $\gamma = 1.00$ all source nodes are allocated the maximum admissible transmission power. Moreover, for $\gamma < 1.00$, w.NBS and MWAD tend to restrict the range of the assigned transmission power for low and medium motion source nodes and their corresponding relay nodes, compared to e.NBS and MWAD. This can be explained from the fact that by using the motion-aware criteria, we intend to favor the clusters in proportion to the amount of motion. So, in order to enhance the video quality of the high motion nodes, the motion-aware criteria increase the transmission power of these nodes and concurrently reduce the transmission power of all other clusters and relay nodes. This increases the energy-per-bit to MAI and noise ratio for the high motion nodes and their relay nodes, while at the same time it reduces it for the other clusters and their corresponding relay nodes.

Network lifetime is one of the most important metrics for the evaluation of a sensor network, due to the fact that it is energy-constrained and that it can fulfill its purpose as long as its sensors are "alive". Several definitions

27

for sensor lifetime have been provided in the literature [3, 51, 52]. According to [51], it is the time until the first sensor is drained of its energy. Figure 4 reveals that the motion-aware criteria use higher transmission power for the high motion source nodes of $C1$ for most (γ, δ) pairs. This observation is more intense for MWAD, which allocates the maximum transmission power to the source nodes of C1 for $\gamma \geq 0.50$. Regarding the transmission power of the relay nodes, Fig. 5 indicates that employing EWAD results in the highest admissible power for R1 (that is committed to C1) for all (γ, δ) pairs. Overall, according to this sensor lifetime definition, the employment of the NBS-based criteria enhances the WVSN lifetime compared to EWAD and MWAD for $\gamma \geq 0.50$.

6.2.3. Video Quality and Power Consumption Tradeoff

Figure 6 illustrates the expected video quality at the receiver versus the total consumed transmitted power in the network. The different values of resulting quality and total transmission power derive from different choices of (γ, δ). To better demonstrate the impact and benefits of power control on the delivered video quality, we compare the PSNR for $\gamma < 1.00$ with the PSNR for $\gamma = 1.00$ (when no power control is applied).

Considering the definition of [52], according to which lifetime is defined as the time until all nodes have been drained of their energy, the following conclusions are drawn. This definition is directly related to the total transmission power consumption, which is illustrated for all criteria in Fig. 6. Regarding the WVSN transmission power consumption, the four criteria use different total transmission power for the different (γ, δ) pairs. A first observation from this figure is that EWAD consumes the highest total transmission power for most γ values, i.e. $\gamma \leq 0.95$, while for $\gamma > 0.95$ e.NBS uses the highest total transmission power. On the other hand, it is evident, that w.NBS requires the lowest total transmission power than all other criteria for all considered (γ, δ) pairs. For $\gamma \geq 0.84$, the total transmission power of MWAD is less than 1 W higher compared to w.NBS total transmission power. Considering all the above observations and the definition of [52], we conclude that w.NBS prolongs the WVSN lifetime. Finally, as previously observed in Fig. 4, it is important to point out that in case we do not apply power control, all source nodes use the highest admissible transmission power. This means that in this case all source nodes will drain their energy at the same time, according to both of the aforementioned lifetime definitions.

From the video quality point of view, as anticipated e.NBS and EWAD

28

favor the low motion nodes by achieving better quality than w.NBS and MWAD can provide for all values of γ. However, with e.NBS a degradation of the quality of videos of the high motion nodes is experienced, when the total transmitted power is higher than 22 W. A slighter degradation of the quality of videos of the high motion nodes is also experienced with EWAD. Particularly, for $\gamma = 0.50$ the PSNR value is 0.42 dB higher for the low motion nodes than it is for $\gamma = 1.00$, while 5.38 W less are spent in total. Moreover, EWAD requires higher total transmission power than e.NBS for most values of (γ, δ). In contrast, the motion-aware criteria offer considerably higher PSNR to high motion nodes for all values of γ when compared with e.NBS and EWAD. Regarding the low and medium motion videos, the performance of w.NBS is inferior to that of e.NBS. However, MWAD enhances the performance for low and medium motion videos compared to w.NBS, since PSNR is improved by 0.27-3.52 dB for all values of γ.

Furthermore, we observe that, when we use the proposed QEPC method, we can achieve similar video quality compared to the case when no power control is applied (i.e. $\gamma = 1.00$), while we consume less transmission power in total. As an illustration of this remark, consider as an example the case of $\gamma = 0.99$ for w.NBS criterion in Fig. 6(b). In this case, w.NBS achieves almost the same video quality for all clusters as it would if no power control were used. Concurrently, 18.25% (namely 4 W) less transmission power is consumed in total. For the same γ, in the case of MWAD criterion (Fig. 6(d)), the expected video quality at the receiver slightly drops, while the transmission power savings are 17.40%. Considering all these observations, we conclude that when power control is omitted ($\gamma = 1.00, \delta = 0.00$), the consumption of the total transmission power is excessive for a rather small video quality gain. Moreover, the prioritized optimization criteria succeed in enhancing the network lifetime in comparison to the other criteria at a rather small expense on the quality performance. Furthermore, w.NBS provides acceptable video quality (namely higher than the minimum quality requirement threshold $PSNR_{\min}$) for all source nodes, even when low transmission power is allocated to both source and relay nodes.

6.2.4. Fairness of the Resulting Video Quality versus Transmission Power

Figure 7 depicts the resulting ϕ versus the total transmission power for all optimization criteria for all considered (γ, δ) values. Juxtaposing the ϕ values of the proposed QEPC method with the values when no power control is applied, we observe that fairness is degraded when no power control is applied.

29

Another observation is that NBS criteria result in more fair resource allocation for the whole WVSN, while consuming less total transmission power compared to the other two criteria for most (γ, δ) pairs. We have to note that for those (γ, δ) pairs that EWAD and MWAD achieve higher ϕ values, the transmission power for NBS-based criteria in most cases is lower. Additionally, an interesting observation is that the NBS-based criteria result in the same or higher ϕ values compared to the other two criteria (for different (γ, δ) values) and for much lower total transmission power. For example, w.NBS achieves $\phi = 0.76$ using 9.20 W, while MWAD achieves the same ϕ value by consuming 14.50 W (57.6% more than w.NBS). Moreover, we observe that the criteria that consider motion-related prioritization have lower levels of fairness. This is due to the fact that in order to provide higher priority to the nodes of higher motion and increase their PSNR values, the resources allocated to those nodes are increased. This results in higher interference to the other WVSN nodes that degrades their end-to-end video quality. Finally, it is obvious that e.NBS and w.NBS achieve higher degree of fairness over the whole WVSN, while consuming less total transmission power compared to EWAD and MWAD criteria.

6.3. Performance of PSO and PSO-RE

As explained in Section 4.3, the PSO-RE algorithm was introduced in [36], achieving superior performance than traditional PSO. In our experimental setting, the dimensions of the underlying optimization problems were $\mathcal{D} = 16$ for Topology I and $\mathcal{D} = 10$ for Topology II. For each problem instance, 30 independent experiments were conducted for both PSO-RE and PSO, in order to extract sound information regarding their performance. We note that in case of a real-time process, only a single experiment is conducted.

Besides convergence speed, we tested the validity of PSO-RE also in terms of solution quality, i.e., the resulting resource allocation. Both PSO and PSO-RE converged to the same optimal solution $\mathcal{F}^*$ with an accuracy of 12 decimals. For all criteria and (γ, δ) values, both algorithms achieved the same solutions, although PSO-RE required far less computational resources. This performance was verified for both Topology I and II.

In Fig. 8, we illustrate an example of convergence speed of the two solvers to the same solution $\mathcal{F}^*$ for e.NBS and w.NBS, for $(\gamma = 0.85, \delta = 0.15)$. We only present the first 100 iterations for visibility issues. At each diagram, the best solution per algorithm iteration is plotted. We can clearly observe that

30

using PSO-RE results in faster detection of $\mathcal{F}^*$, despite the fact that it uses smaller swarm size.

Regarding the swarm size and maximum iterations of the two PSO solvers, it is common practice in metaheuristics to set parameters after a preprocessing phase. In this phase, preliminary experimentation is performed in order to identify proper parameter values. In our case, PSO-RE required significantly lower computational resources than PSO since it is equipped with the estimation scheme described in Section 4.3.2. Nevertheless, determining optimal parameter values for stochastic optimization algorithms is still an open optimization problem itself, while experimental evidence suggests that it is always dependent on the considered optimization problem.

In Table 5, we report the maximum swarm size ($|\mathcal{Q}|$) and maximum number of algorithm iterations ($Iter$) that are required for all (γ, δ) values for the presented results. As observed, the required $|\mathcal{Q}|$ and $Iter$ are not identical for each topology. This is due to the fact that these parameters depend on the dimension of the optimization problem. Also, they depend on the special characteristics of the objective function $\mathcal{F}$, which is not identical for the different network configurations (e.g., there are different numbers of hops per source node).

For Topology I, the maximum number of function evaluations required by PSO-RE (given as the product $|\mathcal{Q}| \cdot Iter$) is 90% lower than the corresponding number required by traditional PSO. For Topology II, PSO-RE requires 88% less function evaluations. To further verify the faster convergence of PSO-RE compared to PSO, as well as the feasibility of the proposed method, we report in Table 5 the average execution time T_{exe} for an experiment on an Intel Core i7-4510U CPU @2.00GHz using Cygwin with 2GB of RAM reserved. As we can see, on average, PSO-RE is 91.91% faster than PSO for Topology I and 89.98% faster for Topology II.

Table 5: Comparison of PSO and PSO-RE for Topology I and II.

	Algorithm	$|\mathcal{Q}|$	$Iter$	$T_{\text{exe}}(sec)$
Topology I	PSO	200	3000	304.56
	PSO-RE	80	650	24.65
Topology II	PSO	50	500	12.47
	PSO-RE	30	100	1.25

31

7. Conclusion

In this paper, we propose an effective methodology for solving the QEPC problem in cooperative multihop WVSNs by jointly allocating the transmission powers to all nodes, the source coding rates to the source nodes and the channel coding rates to all nodes. For this reason, we defined bi-objective optimization criteria. Both e.NBS and w.NBS, are based on the NBS and employ a utility function that reflects the benefit in terms of quality along with the cost in terms of transmission power. We compared the NBS-based criteria with other two criteria, EWAD and MWAD, that aggregate the distortion and the transmission powers of all nodes. More specifically, w.NBS and MWAD are prioritized so as to favor specific WVSN nodes in proportion to the motion level of the recorded scenes. The evaluation results confirmed that the proposed QEPC method achieves to effectively balance the QoS in terms of end-to-end video quality and the total transmission power consumption. Particularly, in many cases, excessive transmission power is used when power control is omitted for a rather small quality gain for certain nodes. This important observation is also verified by the overall fairness assessment results. Concluding, NBS-based criteria that employ the proposed utility function are the prominent choice to effectively balance the video quality fairness and WVSN lifetime tradeoff.

References

[1] I. F. Akyildiz, T. Melodia, and K. R. Chowdhury, "A survey on wireless multimedia sensor networks," *Computer Networks*, vol. 51, no. 4, pp. 921–960, Mar. 2007.

[2] D. G. Costa and L. A. Guedes, "A Survey on Multimedia-Based Cross-Layer Optimization in Visual Sensor Networks," *Sensors*, vol. 11, pp. 5439–5468, 2011.

[3] I. Dietrich and F. Dressler, "On the lifetime of wireless sensor networks," *ACM Transactions Sensor Networks*, vol. 5, no. 1, pp. 5:1–5:39, Feb. 2009.

[4] E. G. Datsika, A. V. Katsenou, L. P. Kondi, E. Papapetrou, and K. E. Parsopoulos, "Priority–based cross–layer optimization for multihop DS–CDMA visual sensor networks," in *Proc. IEEE International Conference on Image Processing*, Orlando, Florida, 2012, pp. 1102–1104.

[5] S. Betz and H.V. Poor, "Energy efficiency in multi-hop CDMA networks: A game theoretic analysis considering operating costs," in *Proc. IEEE International Conference on Acoustics, Speech and Signal Processing*, 2008, pp. 2781–2784.

[6] L. P. Kondi and E. S. Bentley, "Game–Theory–based cross–layer optimization for Wireless DS–CDMA Visual Sensor Networks," *IEEE International Conference on Image Processing*, pp. 4485–4488, 2010.

[7] H. Park and M. van der Schaar, "Bargaining strategies for networked multimedia resource management," *IEEE Transactions on Signal Processing*, vol. 55, no. 2, pp. 3496–3511, July 2007.

[8] A. V. Katsenou, L. P. Kondi, and K. E. Parsopoulos, "Resource Management for Wireless Visual Sensor Networks Based on Individual Video Characteristics," in *Proc. IEEE International Conference on Image Processing*, Brussels, September 2011, pp. 149–152.

[9] U. C. Kozat and I. Koutsopoulos, "Cross-layer design for power efficiency and QoS provisioning in multi-hop wireless networks," *IEEE Transactions on Wireless Communications*, vol. 5, no. 11, pp. 3306–3315, November 2006.

[10] R. Devarajan, S. Jha, U. Phuyal, and V. Bhargava, "Energy-Aware Resource Allocation for Cooperative Cellular Network Using Multi-Objective Optimization Approach," *IEEE Transactions on Wireless Communications*, vol. 11, no. 5, pp. 1797–1807, May 2012.

[11] Q. Ni and C. C. Zarakovitis, "Nash Bargaining Game Theoretic Scheduling for Joint Channel and Power Allocation in Cognitive Radio Systems," *IEEE Journal on Selected Areas in Communications*, vol. 30, no. 1, pp. 70–81, January 2012.

[12] Laura Toni, Thomas Maugey, and Pascal Frossard, "Correlation-aware packet scheduling for multi-camera streaming," in *19th International Packet Video Workshop (PV)*, 2012.

[13] Bo Yang, Yanyan Shen, Gang Feng, and Xinping Guan, "Fair resource allocation using bargaining over OFDMA relay networks," in *Proceedings of the 48th IEEE Conference on Decision and Control, 2009 held*

33

jointly with the 2009 28th Chinese Control Conference, Dec 2009, pp. 585–590.

[14] Y. Shen, G. Feng, B. Yang, and X. Guan, "Fair resource allocation and admission control in wireless multiuser amplify-and-forward relay networks," *IEEE Transactions on Vehicular Technology*, vol. 61, no. 3, pp. 1383–1397, March 2012.

[15] S. Ren and M. van der Schaar, "Pricing and distributed power control in wireless relay networks," *IEEE Transactions on Signal Processing*, vol. 59, no. 6, pp. 2913–2926, June 2011.

[16] N. Feng, S. C. Mau, and N. B. Mandayam, "Pricing and power control for joint network-centric and user-centric radio resource management," *IEEE Transactions on Communications*, vol. 52, no. 9, pp. 1547–1557, Sept. 2004.

[17] J. Nash, "The bargaining problem," *Econometrica*, vol. 18, pp. 155–162, 1950.

[18] K. Pandremmenou, L. P. Kondi, K. E. Parsopoulos, and E. S. Bentley, "Game–theoretic solutions through intelligent optimization for efficient resource management in wireless visual sensor networks," *Sig. Proc.: Image Comm.*, vol. 29, no. 4, pp. 472–493, 2014.

[19] J. Chen and A. L. Swindlehurst, "Applying bargaining solutions to resource allocation in multiuser MIMO–OFDMA broadcast systems," in *IEEE Journal of Selected Topics in Signal Processing*, April 2012, vol. 6, pp. 127–139.

[20] G. Zhang, H. Zhang, L. Zhao, W. Wang, and L. Cong, "Fair resource sharing for cooperative relay networks using nash bargaining solutions," *IEEE Communications Letters*, vol. 13, no. 6, pp. 381–383, June 2009.

[21] H. Yaïche, R. R. Mazumdar, and C. Rosenberg, "A game theoretic framework for bandwidth allocation and pricing in broadband networks," *IEEE/ACM Transaction on Networking*, vol. 8, no. 5, pp. 667–678, Oct. 2000.

[22] A. V. Katsenou, E. G. Datsika, L. P. Kondi, E. Papapetrou, and K. E. Parsopoulos, "Power–Aware QoS enhancement in Multihop DS–CDMA

34

Visual Sensor Networks," in *Proc. of the 18th International Conference on Digital Signal Processing*, Santorini, July 2013.

[23] D. Bertsimas, V. F. Farias, and N. Trichakis, "The price of fairness," *Oper. Res.*, vol. 59, no. 1, pp. 17–31, Jan. 2011.

[24] M. Dianati, X. Shen, and S. Naik, "A new fairness index for radio resource allocation in wireless networks," in *IEEE Wireless Communications and Networking Conference*, March 2005, vol. 2, pp. 712–717 Vol. 2.

[25] G. Tan, *Improving aggregate user utilities and providing fairness in multi-rate wireless LANs*, Ph.D. thesis, Massachusetts Inst. Technol. (MIT), Cambridge, MA, USA, 2006.

[26] H. Park and M. van der Schaar, "Fairness strategies for wireless resource allocation among autonomous multimedia users," *IEEE Trans. on Circuits and Systems for Video Technology*, vol. 20, no. 2, pp. 297–309, Feb. 2010.

[27] H. P. Young, *Equity: In Theory and Practice*, Princeton University Press, Princeton, NJ, 1995.

[28] Y. S. Chan and J. W. Modestino, "A joint source coding-power control approach for video transmission over CDMA networks," *IEEE Journal on Selected Areas in Communications*, vol. 21, no. 10, pp. 1516–1525, 2003.

[29] T. Rapaport, *Wireless Communications Principles and Practice*, Prentice Hall Communications Engineering and Emerging Technologies Series. Prentice Hall, 2nd edition, 2001.

[30] A. Luthra H. Wang, L. P. Kondi and S. Ci, *4G Wireless Video Communications*, John Wiley & Sons, Ltd, 2009.

[31] J. Hagenauer, "Rate-compatible punctured convolutional codes (RCPC codes) and their applications," *IEEE Transactions on Communications*, vol. 36, no. 4, pp. 389–400, April 1988.

[32] T. Wiegand and G. Sullivan, "The H.264/AVC Video Coding Standard Standards in a nutshell," *IEEE Signal Processing Magazine*, vol. 24, no. 2, pp. 148–153, March 2007.

35

[33] L. P. Kondi and A. K. Katsaggelos, "Joint source-channel coding for scalable video using models of rate distortion functions," in *Proc. IEEE International Conference on Acoustics, Speech and Signal Processing*, Salt Lake City, 2001, pp. 1377–1380.

[34] E. S. Bentley, L. P. Kondi, J. D. Matyjas, M. J. Medley, and B. W. Suter, "Spread spectrum visual sensor networks resource management using an end-to-end cross layer design," *IEEE Transactions on Multimedia*, vol. 13, no. 1, pp. 125–131, February 2011.

[35] H. Yang and K. Rose, "Advances in Recursive Per–Pixel End–to–End Distortion Estimation for Robust Video Coding in H.264/AVC," *IEEE Transactions on Circuits and Systems for Video Technology*, vol. 17, no. 7, pp. 845–856, July 2007.

[36] A. V. Katsenou, L. P. Kondi, and K. E. Parsopoulos, "Motion–Related Resource Allocation in Dynamic Wireless Visual Sensor Network Environments," *IEEE Transactions on Image Processing*, vol. 23, no. 1, pp. 56–68, 2014.

[37] K. Binmore, *Playing for Real: A Text on Game Theory*, Oxford University Press, 2007.

[38] J. E. Suris, L. A. DaSilva, Zhu Han, A. B. MacKenzie, and R. S. Komali, "Asymptotic optimality for distributed spectrum sharing using bargaining solutions," *IEEE Transactions on Wireless Communications*, vol. 8, no. 10, pp. 5225–5237, 2009.

[39] K. E. Parsopoulos and M. N. Vrahatis, *Particle Swarm Optimization and Intelligence: Advances and Applications*, Information Science Publishing (IGI Global), 2010.

[40] M. Clerc and J. Kennedy, "The particle swarm-explosion, stability, and convergence in a multidimensional complex space," *IEEE Trans. Evol. Comput.*, vol. 6, no. 1, pp. 58–73, 2002.

[41] S. Kiranyaz, T. Ince, and M. Gabbouj, *Multidimensional Particle Swarm Optimization for Machine Learning and Pattern Recognition*, (Adaptation, Learning, and Optimization). Springer, 2013.

[42] A. E. Olsson, *Particle Swarm Optimization: Theory, Techniques and Applications*, Nova Science Publishers, 2011.

[43] M. Clerc, *Particle Swarm Optimization*, John Wiley & Sons, 2013.

[44] I. C. Trelea, "The particle swarm optimization algorithm: convergence analysis and parameter selection," *Information Processing Letters*, vol. 85, no. 6, pp. 317–325, 2003.

[45] F. van den Bergh and A. P. Engelbrecht, "A study of particle swarm optimization particle trajectories," *Information Sciences*, vol. 176, no. 8, pp. 937–971, 2006.

[46] V. Kadirkamanathan, K. Selvarajah, and P.J. Fleming, "Stability analysis of the particle dynamics in particle swarm optimizer," *IEEE Transactions on Evolutionary Computation*, vol. 10, no. 3, pp. 245–255, June 2006.

[47] M. Jiang, Y. P. Luo, and S. Y. Yang, "Stochastic convergence analysis and parameter selection of the standard particle swarm optimization algorithm," *Information Processing Letters*, vol. 102, no. 1, pp. 8–16, 2007.

[48] R. V. Kulkarni and G. K. Venayagamoorthy, "Particle Swarm Optimization in Wireless-Sensor Networks: A Brief Survey," *IEEE Transactions on Systems, Man, and Cybernetics, Part C: Applications and Reviews*, vol. 41, no. 2, pp. 262–267, March 2011.

[49] K. E. Parsopoulos and M. N. Vrahatis, *Multiobjective Particle Swarm Optimization Approaches, Multi-Objective Optimization in Computational Intelligence: Theory and Practice*, Information Science Publishing (IGI Global), 2008.

[50] R. Jain, D. M. Chiu, and W. Hawe, "A Quantitative Measure of Fairness and Discrimination for Resource Allocation in Shared Systems," *DEC Research Report TR–301*, 1984.

[51] J.-H. Chang and L. Tassiulas, "Energy conserving routing in wireless ad-hoc networks," in *Proc. IEEE Nineteenth Annual Joint Conference of the IEEE Computer and Communications Societies INFOCOM*, 2000, vol. 1, pp. 22–31.

[52] D. Tian and N. D. Georganas, "A Coverage-Preserving Node Scheduling Scheme for Large Wireless Sensor Networks," in *Proceedings of the 1st ACM international workshop on Wireless sensor networks and applications.* 2002, pp. 32–41, ACM Press.
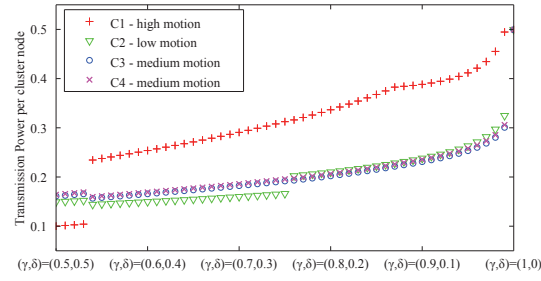
(a) Results for e.NBS criterion.
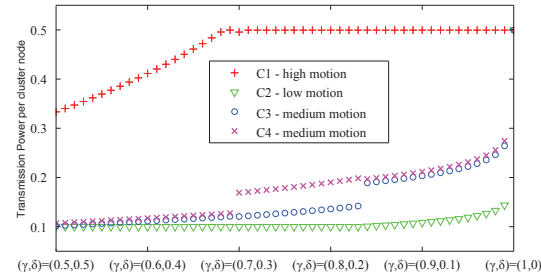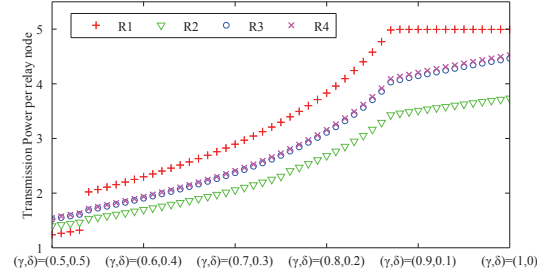
(b) Results for w.NBS criterion.
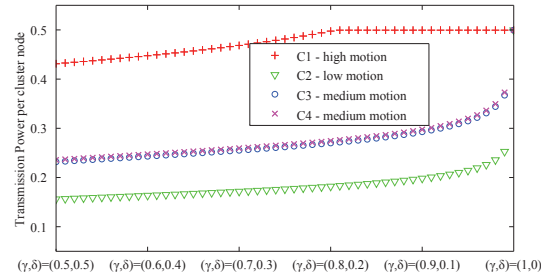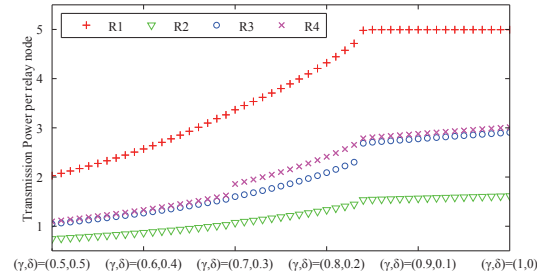
(c) Results for EWAD criterion.
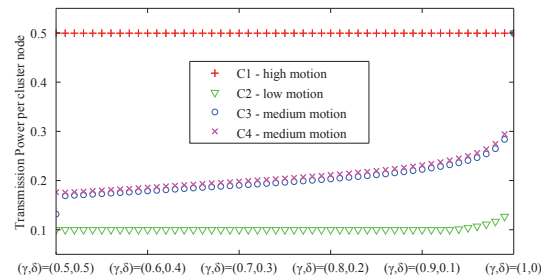
(d) Results for MWAD criterion.

39

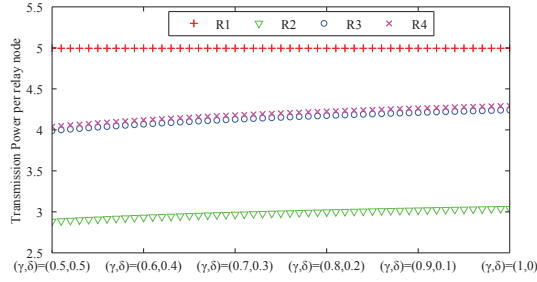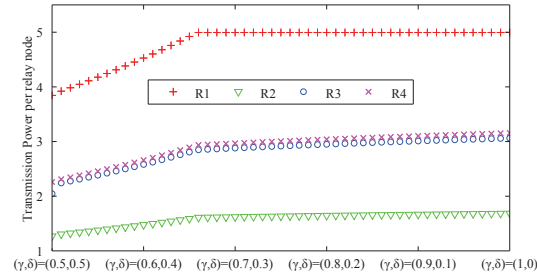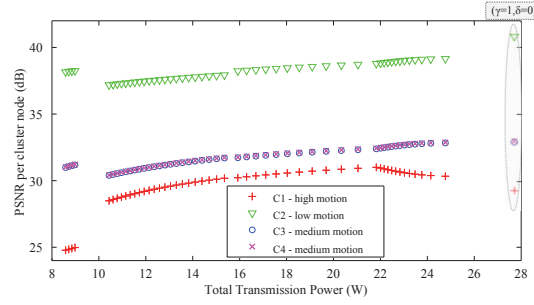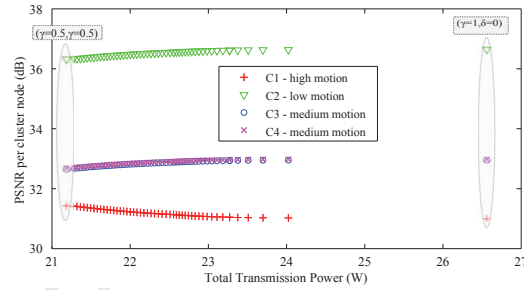Figure 4: Transmission Power per Cluster node versus different (γ, δ) pairs for all three criteria.

(a) Results for e.NBS criterion.

(b) Results for w.NBS criterion.

(c) Results for EWAD criterion.

(d) Results for MWAD criterion.

Figure 5: Transmission Power per Relay node versus different (γ, δ) pairs for all criteria.

(a) Resulting Quality versus Total Transmission Power for e.NBS.
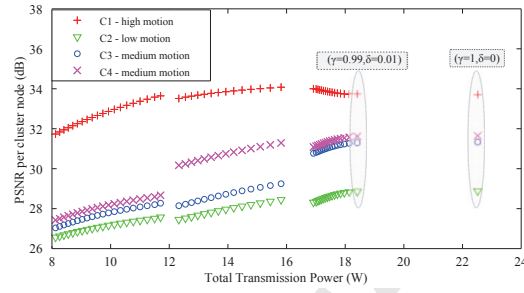
(b) Resulting Quality versus Total Transmission Power for w.NBS.

(c) Resulting Quality versus Total Transmission Power for EWAD.
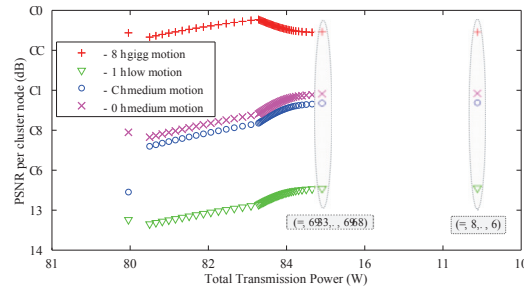
(d) Resulting Quality versus Total Transmission Power for MWAD.

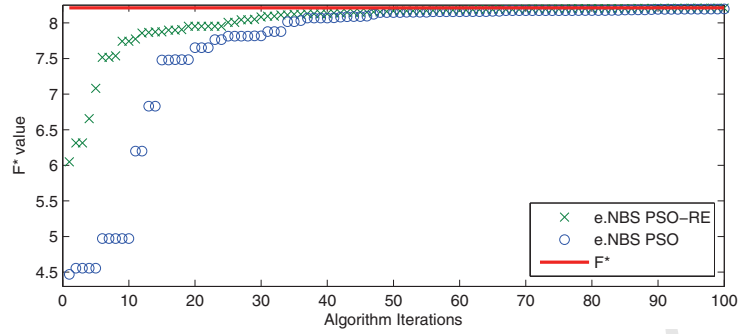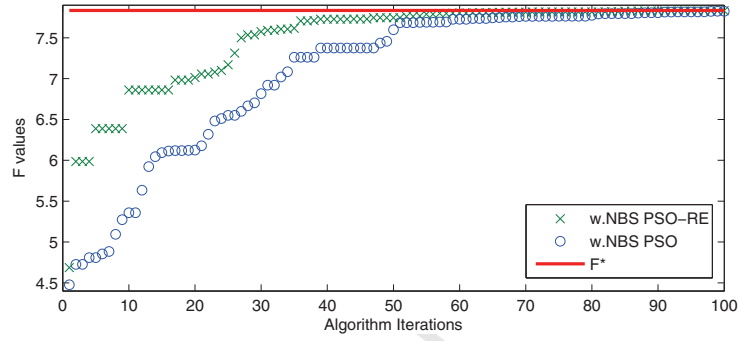Figure 6: Video Quality-Transmission Power tradeoff per cluster using all optimization criteria.
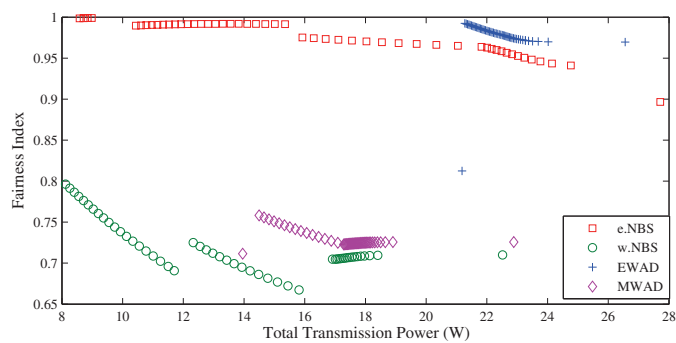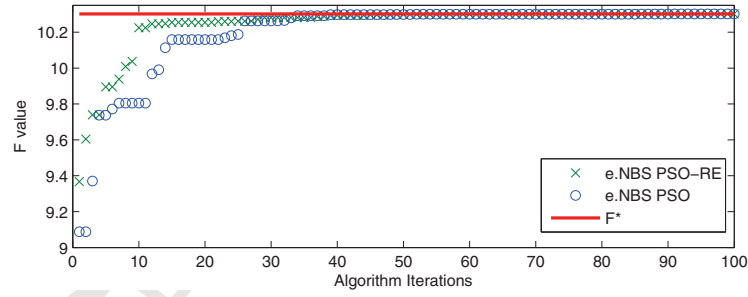
Figure 7: Fairness index ϕ versus the Total Transmission Power for all criteria.
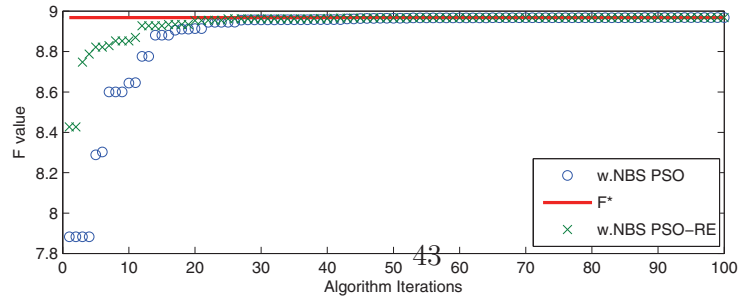
(a) Topology I with e.NBS for $\gamma = 0.85$.

(b) Topology I with w.NBS for $\gamma = 0.85$.

(c) Topology II with e.NBS for $\gamma = 0.85$.

(d) Topology II with w.NBS for $\gamma = 0.85$.

Figure 8: Comparison of the convergence of the optimization algorithms.

Eftychia Datsika received her B.Sc. and M.Sc. degree in Computer Science from
 the Computer Science Department, University of Ioannina, Greece in 2010 and
2012, respectively. She is working as an Early Stage Researcher in IQUADRAT
Informatica S.L., Spain. Her current research interests lie in the areas of
Long Term Evolution Advanced networks and Device-to-Device communication.

Angeliki V. Katsenou is a Marie Sklodowska-Curie Experienced Research Fellow
of the PROVISION ITN project and she is with the Visual Information Lab
at the University of Bristol. She received her M.Eng. in Electrical and Computer
Engineering and the M.Sc. degree in Signal and Image Processing from the
University of Patras, Greece, in 2004 and 2007, respectively. She
obtained her Ph.D. degree in the Department of Computer Science
and Engineering, University of Ioannina, Greece. She has experience in
several EC-funded ICT projects. Her research interests include perceptual
video analysis and coding, wireless visual sensor networks, resource allocation
algorithms, and game-theoretic approaches in multimedia communication
systems.

Lisimachos P. Kondi received the Diploma in electrical engineering from the Aristotle
University of Thessaloniki, Greece, in 1994 and the M.S. and Ph.D. degrees in electrical
and computer engineering from Northwestern University, Evanston, IL, USA, in 1996 and 1999,
 respectively. He is currently an Associate Professor in the Department of Computer Science
and Engineering, University of Ioannina, Greece. He was previously with the faculty of the
University at Buffalo, The State University of New York and has held summer appointments at
the Naval Research Laboratory (Washington, DC) and the Air Force Research Laboratory (Rome, NY).
 His research interests are in the general areas of signal and image processing and communications,
including image and video compression and transmission over wireless channels and the Internet, sparse
representations and compressive sensing, super-resolution of video sequences, and shape coding.

 Dr. Kondi
is a co-author of 33 journal papers and 77 conference papers. He is also a co-author of a book entitled
"4G Wireless Video Communications" (Wiley, 2009). He has been an Associate Editor of the IEEE Signal

Processing Letters (2008-2012), the EURASIP Journal on Advances in Signal Processing (2005-present), and
the International Journal of Distributed Sensor Networks (2013-2015). He was Technical Program Committee
(TPC) Chair of the International Conference on Digital Signal Processing (DSP), Santorini, Greece, 2013,
and will serve as Technical Program Committee Chair of the IEEE International Conference on Image Processing
(ICIP), Athens, Greece, 2018.

Evangelos Papapetrou received the Diploma in Electrical and Computer Engineering and the Ph.D. in Telecommunications
from the Department of Electrical and Computer Engineering, Aristotle University of Thessaloniki (AUTh) in 1998 and
2003, respectively. He is an assistant professor in the Department of Computer Science & Engineering, University of
Ioannina since 2011. His research interests include networking in wireless and mobile environments such as mobile
ad-hoc, opportunistic and satellite networks, video transmission, quality of service (QoS) and network coding. More
information is available at http://www.cse.uoi.gr/~epap.

Dr Konstantinos Parsopoulos serves as Assistant Professor on Optimization and Modeling with the Department of Computer
Science and Engineering, University of Ioannina, Greece. He has co-authored 1 book and published 100 papers in
scientific journals, conferences, and edited volumes. His research has received more than 3000 citations. He
has served as board member in 9 international journals and committee member in numerous international conferences.
Also, he has been an external reviewer for the Wiener Wissenschafts-, Forschungs- und Technologiefonds (WWTF) in Austria, the Portuguese Foundation for Science and Technology (FCT), and the South Africa's National Research Foundation (NRF), as well as
for more than 70 journals.